**Proceedings of the ASME 2022
International Mechanical Engineering Congress and Exposition
IMECE2022
October 30–November 3, 2022, Columbus, OH**

IMECE2022-95425

ADAPTIVE ASSIST AS NEEDED CONTROL STRATEGY FOR A LOWER LIMB EXOSKELETON

Shubham Kumbhar[1], Vivek Sangwan[1,*]

[1]Department of Mechanical Engineering, Indian Institute of Technology Bombay, Mumbai, Maharashtra, India

ABSTRACT

Robotic Exoskeletons for legs are able to act as excellent evaluation as well as training devices while reducing physical effort that a therapist needs to expend. For such exoskeletons, assist as needed control strategies are advantageous because these lead to active participation from the user. One such strategy is based on Force Fields where the controller creates a virtual force field around the foot of the user to aid the user's leg motion. Force field controllers (FFC) presented in literature require the knowledge of parameters such as length, mass, position of center-of-mass and moment of inertia for the combined human-exoskeleton system. This paper presents an "adaptive" assist as needed control strategy that creates a virtual force field similar to the FFC without using any prior knowledge of human inertial parameters like mass, the moment of inertia, the position of COM, etc. A lyapunov stability proof for the proposed controller is also presented along with simulation results demonstrating the controller.

Keywords: Adaptive Control, Force Field Controller, Lyapunov Stability

1. INTRODUCTION

Lower Limb Exoskeletons have proved to be extensively valuable for human gait rehabilitation [1]. Robotic rehabilitation has many advantages over manual rehabilitation, such as reduced dependence on clinical staff and delivery of controlled repetitive training using robotics at a reasonable cost [2–4]. Such exoskeletons can be classified as (a) *Passive* [5, 6]: where the exoskeleton does not have any actuator and the user applies forces to move the leg and the exoskeleton, and (b) *Active* [1, 2]: where the exoskeleton has actuators and is able to apply forces to drive the leg along with itself. Several control related aspects for these exoskeletons have been researched. An interesting aspect is the determination of the intention of the user for which various biological signals like the surface electromyographic signals or the brain signals are used for determining the intent of the user [7]. Another important aspect is the translation of the users' intentions into torques or forces applied by the controller. An interesting study along these lines is presented in [8] where EMG signals are used to implement an adaptive impedance controller for upper limb exoskeletons. An adaptive controller is presented in [9] which provides a continuous adaptation of controller gains to adapt between passive and active-assistive control mode, depending on the user's performance. The simplest type of controllers are those that follow a predetermined trajectory or a predetermined force. Many of the older designs such as [2] initially employed control strategies that move a user along predetermined patterns and do not allow the user to participate in the gait training actively. This also causes failure to adapt to changes in the movement patterns. It is much better to have a flexible control strategy that allows users to actively modify their movement patterns and assists only when required.

An assist as needed control strategy was used in [1]. Here they used a force-field controller which creates a desired force field around the moving foot and directs it towards the desired gait trajectory. The goal of this controller is not to track a desired trajectory rather it assists or resists the motion of the foot depending on its position relative to the desired trajectory. When the foot is close to the desired trajectory the forces applied by the exoskeleton are small and these forces are high when the deviation from the desired trajectory is higher. Such a control strategy leads to active participation from the users side. It was demonstrated by [1, 10] that such assist as needed (ANN) strategies can lead to more adaptation in walking pattern and more efficient gait training. When practically implementing these control strategies, measurement of inertial parameters like mass, moment of inertia, etc. are required. It is difficult to measure these parameters accurately. Also, every time a new user comes in, all the measurements need to be repeated. A model reference adaptive control was proposed in [11] that achieves simultaneous control of the exoskeleton as well as estimates the plant parameters. This paper addresses this problem by designing an adaptive assist as needed control strategy that creates a virtual field similar to the Force Field controller used by [1] for gait training but without

*Corresponding author: vivek.sangwan@iitb.ac.in

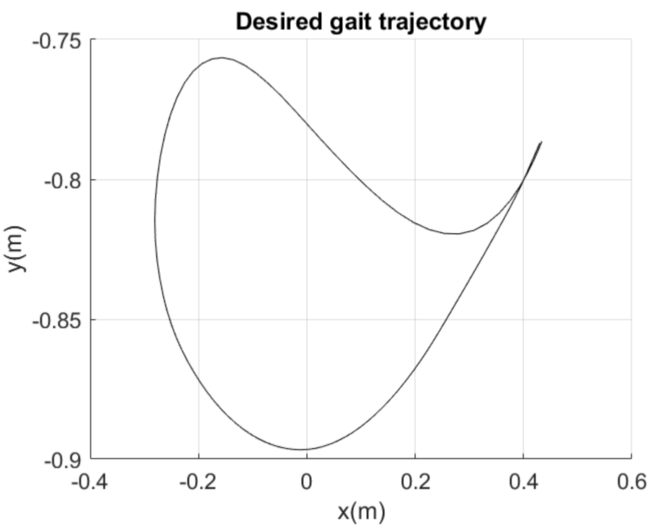

FIGURE 1: DESIRED GAIT TRAJECTORY HERE, X AND Y GIVE THE POSITION OF THE FOOT WITH RESPECT TO AN INERTIAL FRAME, FRAME 0, FIXED TO THE HIP. REFER FIG. 3
for a pictorial representation of frames

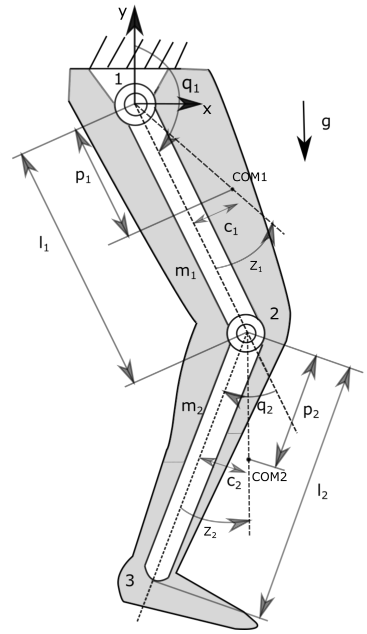

FIGURE 2: SCHEMATIC OF THE LEG MODEL. HERE, l_1, m_1 AND I_1 ARE THE LENGTH, MASS AND MOMENT OF INERTIA ABOUT COM OF THE THIGH LINK. SIMILARLY, l_2, m_2 AND I_2 ARE THE LENGTH, MASS AND MOMENT OF INERTIA ABOUT COM OF THE SHANK LINK

any knowledge of the parameters of the users body except the lengths of thigh and shank segments. Using Lyapunov's method the stability of the proposed adaptive controller is established.

This paper is organized as follows. Dynamic modelling of the exoskeleton is presented in Section 2. This is followed by a description of the Force Field controller and proposed adaptation law along with its lyapunov stability analysis in Section 3. Finally results and conclusions are presented in Section 4.

2. DYNAMIC MODELLING OF THE SYSTEM

This section presents a simple two-link dynamic model of a user wearing an exoskeleton. The system consists of two parts, the exoskeleton and the user attached to the exoskeleton. The exoskeleton drives the user's leg according to a control strategy. In the present case, it creates a virtual force field around the foot and assists the leg when needed. Figure 1 shows the average walking gait trajectory of a healthy human which is used as a desired trajectory [12]. While modelling, we consider the thigh and the thigh link of exoskeleton as one rigid thigh link and similarly the shank and the shank link of exoskeleton as one rigid shank link. Therefore, the dynamic model consists of two rigid planar links as the thigh and shank link and two revolute joints representing the hip and the knee joints. Figure 2 gives a pictorial description of the assumed model. The angles q_1 and q_2 give the angular positions of the links and the convention used for angles is clockwise positive. The following assumptions are made while dynamic modelling of the exoskeleton: (a) The motion takes place in the sagittal plane only, (b) the hip joint is assumed quasi-static (very small and slow motions are assumed for the hip) and, (c) the revolute joints are friction-less. To have a more generalised dynamic model, we consider that the centers-of-mass (COM) of the thigh and shank segment can be located anywhere on the links and not necessarily on the line joining the two revolute joints at the end of the links. The location of these COMs is specified by two variables c_i and p_i, $i = 1, 2$ as shown in Fig. 2. c_1 and p_1 are the distances of COM of thigh link from the hip joint perpendicular to and along the link respectively. Similarly, c_2 and p_2 are the distances of COM of shank link from the knee joint perpendicular to and along the link respectively. z_1 is the angle between the thigh link and the line joining the hip joint and the COM of thigh link. Similarly, z_2 is the angle between the shank link and the line joining the knee joint and the COM of shank link. These angles are depicted in Fig. 2 and are given by:

$$z_1 = \tan^{-1}\left(\frac{c_1}{p_1}\right) \quad z_2 = \tan^{-1}\left(\frac{c_2}{p_2}\right). \tag{1}$$

Using Euler Lagrangian approach, we get the following dynamic equations of the system:

$$\begin{aligned}\boldsymbol{\tau}_1 = {} & [(I_1 + I_2 + m_1 l_{c_1}^2 + m_2 l_{c_2}^2 + m_1 l_1^2 \\ & + 2m_2 l_1 l_{c_2} \cos(q_2 - z_2))\ddot{q}_1 + (I_2 + m_2 l_{c_2}^2 \\ & + m_2 l_1 l_{c_2} \cos(x_2 - z_2))\ddot{q}_2 \\ & - m_2 g l_{c_2} \sin(q_1 + q_2 - z_2) - m_2 l_1 g \sin q_1 \\ & - m_1 g l_{c_1} \sin(q_1 - z_1) - m_2 l_1 l_{c_2} \dot{q}_2{}^2 \sin(q_2 - z_2) \\ & - 2m_2 l_1 l_{c_2} \dot{q}_1 \dot{q}_2 \sin(q_2 - z_2)]\hat{\boldsymbol{k}},\end{aligned} \tag{2}$$

$$\begin{aligned}\boldsymbol{\tau}_2 = {} & [(I_2 + m_2 l_{c_2}^2)(\ddot{q}_1 + \ddot{q}_2) \\ & + m_2 l_1 l_{c_2} \cos(q_2 - z_2)\ddot{q}_1 - m_2 g \sin(q_1 + q_2 - z_2) \\ & - m_2 l_1 \dot{q}_1{}^2 l_{c_2} \sin(q_2 - z_2)]\hat{\boldsymbol{k}}.\end{aligned} \tag{3}$$

Here, l_{c1} and l_{c2} are the distance of the COM of the thigh link from the hip joint and COM of the shank link from the knee joint respectively. These equations can be represented in the

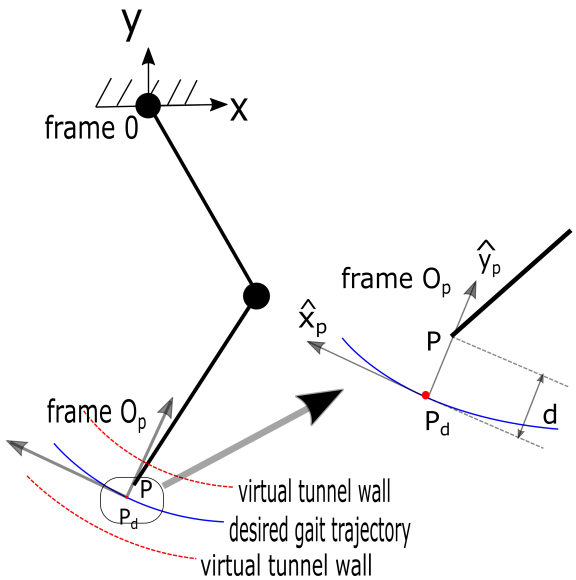

FIGURE 3: PICTORIAL DESCRIPTION OF FRAME-0 AND FRAME O_p

matrix form as Here, $\tau_m = [\tau_1, \tau_2]^T$ and $q = [q_1, q_2]^T$. Also τ_1 and τ_2 are the torques applied by actuators at the hip and knee joint respectively. **M** is the mass matrix, matrix **C** contains the Coriolis and centripetal terms and matrix **G** contains the gravity terms. This equation is in the joint space. We will transform this equation to the task space where the state of the system is given by **x**, the coordinates of the end point of the shank link or the foot in frame-0. Frame-0 is a fixed frame at the hip joint as shown in Fig. 3. With the help of Jacobian matrix, $\boldsymbol{J}$, we can rewrite the equation in the task space. We use the following transformations for getting the task space equations [13]:

$$\begin{aligned} &A_x(q) = J^{T^{-1}} M(q) J^{-1} \qquad \tau = J^T F_0 \\ &H_x(\dot{q}, q) = J^{T^{-1}} C(\dot{q}, q) J^{-1} - A_x(q) \dot{J} J^{-1} \\ &G_x = J^{T^{-1}} G(q) \end{aligned} \tag{4}$$

where $\boldsymbol{x}, \dot{\boldsymbol{x}}$ and $\ddot{\boldsymbol{x}}$ are the position, velocity and acceleration of the foot with respect to the frame 0. $\boldsymbol{F_0}$ is the effective control force acting on the foot. We have assumed that the links do not reach a singularity position which takes place when $q_2 = 0$ and this can be ensured by making sure that the exoskeleton if fixed to the leg such that even when the leg is straight the exoskeleton has a slight bend at its knee. Now let us consider another fixed frame O_p, as shown in Fig. 3, with its one axis($\hat{\boldsymbol{t}}$) tangential to the desired trajectory along the forward direction which is anticlockwise in nature and the other axis($\hat{\boldsymbol{n}}$) is obtained by rotating $\hat{\boldsymbol{t}}$ clockwise by an angle of 90 degrees. The origin of this frame is at the foot of the perpendicular from the current foot position to the desired trajectory. These directions are as shown in the Fig. 4. Now let the acceleration and velocity of the foot in frame O_p be $\boldsymbol{a_m}$ and $\boldsymbol{v_m}$ respectively. These variables can be given by:

$$v_m = \begin{bmatrix} v_t \\ v_n \end{bmatrix} = R^{-1}\dot{x} \qquad and \qquad v_n = \dot{d} \tag{5}$$

$$a_m = \dot{v}_m = \begin{bmatrix} \dot{v}_t \\ \dot{v}_n \end{bmatrix} = R^{-1}\ddot{x} \tag{6}$$

$\boldsymbol{R}$ is the rotation matrix from frame 0 to frame O_p and d is the perpendicular distance between foot and the desired gait trajectory. Note d can be positive or negative depending on the position of the foot with respect to frame O_p. Using Eq. 5 and Eq. 6 we can rewrite the dynamics equations as:

$$A_x R \dot{v}_m + H_x R v_m + G_x = RF \tag{7}$$

$$R^{-1} A_x R \dot{v}_m + R^{-1} H_x R v_m + R^{-1} G_x = F \tag{8}$$

$$A \dot{v}_m + H_p v_m + G_p = F \tag{9}$$

Equations in terms of foot coordinates are used to prove the Lyapunov stability of the controller in the subsequent sections. The controller design and Lyapunov stability proofs are shown in the next section.

3. CONTROLLER DESIGN

This section presents an adaptive assistance as needed controller. This controller achieves two objectives, (a) creates a force field around the foot of the user, similar to one in [1], and (b) does not require prior information of a set of parameters of the exoskeleton and user. The parameters which have been considered to be unknown are mass, inertia, location of COMs of both the links and the acceleration due to gravity.

The goal of Force Field Controller(FFC) is to create a force field around the foot and also to provide damping forces to stabilize it. This field results in a 'virtual tunnel' around the desired trajectory in the sagittal plane. Figure 4 shows a virtual tunnel around a desired trajectory. The width of the tunnel can be adjusted and used to control the level of assistance to be provided. As shown in Fig. 4, a combination of two perpendicular forces, $\mathbf{F_t}$ and $\mathbf{F_n}$ acts on the foot depending on the position of the foot with respect to the tunnel and the desired trajectory. $\mathbf{F_t}$ helps in moving the foot along the direction of the desired trajectory and $\mathbf{F_n}$ helps in preventing the foot from moving too far away from the desired trajectory. Let P be the current position of the foot and P_d be the point closest to P on the desired trajectory. As shown in Fig 4, $\mathbf{F_n}$ acts along a unit normal vector from P to P_d. $\mathbf{F_t}$ acts along $\hat{\mathbf{t}}$, unit tangential vector at P_d along the desired trajectory in the forward direction. The tangential force $\mathbf{F}_t$ is given by:

$$F_t = \begin{cases} K_{ft}\hat{t} & |d|/D_t \leq 1, \\ 0 & otherwise, \end{cases} \tag{10}$$

where K_{ft} and D_t are constants. K_{ft} can be changed to control the tangential force and D_t can be used to control the width of the tunnel on both sides of the desired trajectory. The tangential force, $\mathbf{F_t}$ acts only when the foot position is inside the tunnel. The goal is to apply a tangential force only when the foot position is near the desired trajectory. The normal force $\mathbf{F}_n$ is given by:

$$F_n = -(d/D_n)^n)\hat{n} = -K_n d^n \hat{n} \tag{11}$$

D_n is a constant and n is an odd natural number. D_n is the perdendicular distance $|d|$ when $\mathbf{F_n}$=1$\hat{\boldsymbol{n}}$ N. The nature of this force is such that it always acts towards the desired trajectory,

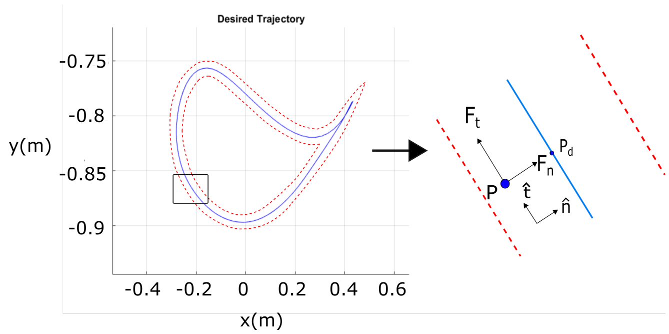

FIGURE 4: CARTESIAN PLOT OF THE DESIRED TRAJECTORY AND TUNNEL WALLS WITH ORIGIN AT THE HIP.BLUE SOLID LINE REPRESENTS DESIRED TRAJECTORY AND THE RED SOLID LINE REPRESENTS TUNNEL WALLS. N IS THE POINT CLOSEST TO P ON THE DESIRED TRAJECTORY. F_T AND F_N ACT AT POINT P

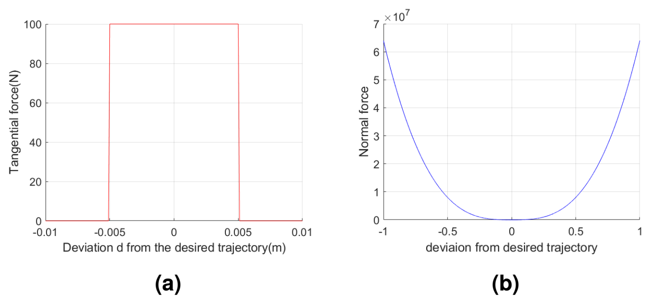

FIGURE 5: (*a*) TANGENTIAL FORCE VARIATION WITH *d* (*b*) NORMAL FORCE VARIATION WITH *d*

along $\hat{\mathbf{n}}$ to move the foot towards it. $\mathbf{F_n}$ is minimum when P is on the desired trajectory and it increases as d increases further. Damping force $\mathbf{F_d}$ is used to control the speed of the foot in $\hat{\mathbf{t}}$ and $\hat{\mathbf{n}}$ directions. It is given by:

$$\boldsymbol{F}_{\mathrm{d}} = F_{\mathrm{dt}}\hat{\boldsymbol{t}} + F_{\mathrm{dn}}\hat{\boldsymbol{n}} \tag{12}$$

F_{dt} and F_{dn} are the damping forces in $\hat{\mathbf{t}}$ and $\hat{\mathbf{n}}$ directions respectively. These are given by:

$$F_{\mathrm{dn}} = -K_{\mathrm{dn}}v_{\mathrm{n}} \tag{13}$$

$$F_{\mathrm{dt}} = \begin{cases} -K_{\mathrm{dt}}v_{\mathrm{t}} & d/D_{\mathrm{t}} \leq 1 \\ 0 & otherwise \end{cases} \tag{14}$$

K_{dt} and K_{dn} are damping constants. v_t and v_n are velocities of the point P in frame O_p. Assistance for moving along the desired trajectory by the controller is provided only when the point P is inside the virtual tunnel. Whenever the point P goes outside the tunnel $\mathbf{F_t}$ stops acting. The controller applies the normal force required to bring the foot close to desired trajectory depending on the distance d. When the foot is close to the desired trajectory small magnitude normal forces are applied meaning the assistance given is less. The magnitude of this force can be controlled using the parameter D_n. In this way, assistance by the FFC is only provided when required depending on the position $\mathbf{P}$ of the foot. Total force $\boldsymbol{F_{total}}$ acting on the foot is given by:

$$\boldsymbol{F_{total}} = \boldsymbol{F}_{\mathrm{t}} + \boldsymbol{F}_{\mathrm{n}} + \boldsymbol{F}_{\mathrm{d}} \tag{15}$$

We want the controller to create the force field $\boldsymbol{F_{total}}$ around the foot of the user. We can rewrite the force field in O_p, in the following matrix form:

$$\boldsymbol{F_{total}} = \begin{bmatrix} \phi(d)(K_{ft} - K_{dt}v_t) \\ -K_n d^n - K_{dn}\dot{d} \end{bmatrix} \tag{16}$$

Here function ϕ is defined as:

$$\phi(d) = \begin{cases} 1 & 0 \leq |d| \leq D_t \\ 0 & otherwise \end{cases} \tag{17}$$

Now let us move on to proving the Lyapunov stability if the controller assuming we have prior knowledge of the parameters of the system. When there is no user activity, the controller will simply guide the foot to the desired trajectory such that the following conditions hold:

$$d \to 0 \qquad \dot{d} \to 0 \qquad v_t \to c = \frac{K_{ft}}{K_{dt}} \tag{18}$$

We can derive our control strategy using these equations as the steady state operating conditions and also keeping in mind that the required force field around the foot is generated. Let us define a vector $\mathbf{p}$ as:

$$\boldsymbol{p} = \begin{bmatrix} v_t - c \\ \dot{d} \end{bmatrix} \tag{19}$$

Also it can be seen that

$$\boldsymbol{p} = \boldsymbol{v_m} - \begin{bmatrix} c \\ 0 \end{bmatrix} \qquad \dot{\boldsymbol{p}} = \dot{\boldsymbol{v}}_{\boldsymbol{m}} \tag{20}$$

Lets choose the Lyapunov function as:

$$V(\boldsymbol{p}, d) = \frac{1}{2}\boldsymbol{p}^T \boldsymbol{A} \boldsymbol{p} + \frac{1}{n+1}K_n d^{n+1} \tag{21}$$

Now V is a positive definite function with $V(\mathbf{0}, 0) = 0$. Differentiating the function we get:

$$\begin{aligned} \dot{V} &= \boldsymbol{p}^T \boldsymbol{A} \dot{\boldsymbol{p}} + \frac{1}{2}\boldsymbol{p}^T \dot{\boldsymbol{A}} \boldsymbol{p} + K_n d^n \dot{d} \\ &= \boldsymbol{p}^T \boldsymbol{A} \dot{\boldsymbol{v}}_{\boldsymbol{m}} + \frac{1}{2}\boldsymbol{p}^T \dot{\boldsymbol{A}} \boldsymbol{p} + K_n d^n \dot{d} \\ &= \boldsymbol{p}^T(\boldsymbol{F} - \boldsymbol{H_p}\boldsymbol{v}_m - \boldsymbol{G_p}) + \frac{1}{2}\boldsymbol{p}^T \dot{\boldsymbol{A}} \boldsymbol{p} + K_n d^n \dot{d} \\ &= \boldsymbol{p}^T\left(\boldsymbol{F} - \boldsymbol{H_p}\begin{bmatrix} c \\ 0 \end{bmatrix} - \boldsymbol{G_p}\right) + \frac{1}{2}\boldsymbol{p}^T(\boldsymbol{A} - 2\boldsymbol{H_p})\boldsymbol{p} + K_n d^n \dot{d} \end{aligned}$$

Now by the fact that rate of change of kinetic energy is equal to the work done by external conservative and non-conservative forces we have that $\boldsymbol{A} - 2\boldsymbol{H_p}$ is a skew symmetric matrix [14] and for any vector $\mathbf{w}$.

$$\boldsymbol{w}^T(\boldsymbol{A} - 2\boldsymbol{H_p})\boldsymbol{w} = 0 \tag{22}$$

The control strategy to use is:

$$F = \boldsymbol{H_p}\begin{bmatrix} c \\ 0 \end{bmatrix} + \boldsymbol{G_p} + \boldsymbol{F_{total,O_p}} \tag{23}$$

$$F = \boldsymbol{H_p}\begin{bmatrix} c \\ 0 \end{bmatrix} + \boldsymbol{G_p} + \begin{bmatrix} \phi(d)(K_{ft} - K_{dt}v_t) \\ -K_n d^n - K_{dn}\dot{d} \end{bmatrix} \tag{24}$$

Using this as the control strategy we have:

$$\dot{V}(\boldsymbol{p}, d) = -K_{dt}\phi(d)(v_t - c)^2 - K_{dn}\dot{d}^2$$
$$= -\boldsymbol{p}^T \begin{bmatrix} K_{dt}\phi(d) & 0 \\ 0 & K_{dn} \end{bmatrix} \boldsymbol{p}$$

It can be seen that $\dot{V}(\boldsymbol{p}, d)$ is a negative semi-definite and so the states of the system will converge to the largest invariant set given by $\boldsymbol{p} = 0$ and $\dot{d} = 0$. This also proves that the system is stable and all the states including d will remain bounded.
The control law is given by:

$$\boldsymbol{F} = \boldsymbol{H_p} \begin{bmatrix} c \\ 0 \end{bmatrix} + \boldsymbol{G_p} + \begin{bmatrix} \phi(d)(K_{ft} - K_{dt}v_t) \\ -K_n d^n - K_{dn}\dot{d} \end{bmatrix} \quad (25)$$

The parameters are as defined in the previous section. $\boldsymbol{G_p}$ is the gravity compensation and $\boldsymbol{H_p}$ is partial compensation of the centrifugal and Coriolis terms of the dynamic equations. This equation can also be written as:

$$\boldsymbol{F} = \boldsymbol{Ya} + \begin{bmatrix} \phi(d)(K_{ft} - K_{dt}v_t) \\ -K_n d^n - K_{dn}\dot{d} \end{bmatrix} = \boldsymbol{Ya} + \boldsymbol{F_{total}} \quad (26)$$

Here $\mathbf{Y}$ is a 2×8 matrix and $\boldsymbol{a}$ an 8×1 vector consisting of unique mathematical combinations of the inertial parameter of the system and acceleration due to gravity. The mathematical expression of $\mathbf{a}$ is given by Eq. 27. Our current controller creates the desired force field around the foot but $\boldsymbol{a}$ matrix in the control law requires the knowledge of system parameters. Now, in the following paragraphs of the section we will assume that the matrix $\boldsymbol{a}$ is not known and will derive an adaptation law using Lyapunov stability analysis that will continuously provide alternate values of $\boldsymbol{a}$ to satisfy the role of the controller.

$$\begin{aligned} \boldsymbol{a} = \begin{bmatrix} a_1 & a_2 & a_3 & a_4 & a_5 & a_6 & a_7 & a_8 \end{bmatrix}^T \\ a_1 = m_2 l_{c_2} \cos(z_2) \\ a_2 = m_2 l_{c_2} \sin(z_2) \\ a_3 = I_2 + m_2 l_{c_2}^2 \\ a_4 = I_1 + I_2 + m_1 l_{c_1}^2 + m_2 l_{c_2}^2 + m_2 l_1^2 \\ a_5 = m_2 g l_{c_2} \cos(z_2) \\ a_6 = m_2 g l_{c_2} \sin(z_2) \\ a_7 = m_1 g l_{c_1} \sin(z_1) \\ a_8 = m_2 g l_1 + m_1 g l_{c_1} \cos(z_1) \end{aligned} \quad (27)$$

The parameters which have been considered to be unknown are mass, inertia, location of COMs of both the links and the acceleration due to gravity. Instead of deriving the adaptation law for individual parameters, we consider a unique combination of these as unknown variables. This idea of linearizing the compensation terms is taken from [14]. The parameter vector $\mathbf{a}$ is considered to be unknown and it is substituted with an estimate by the adaptation law, $\hat{\boldsymbol{a}}$, in the control law given by Eq. 26 for best possible cancellation of the non linear terms. Therefore, the control law becomes:

$$\boldsymbol{F} = \boldsymbol{Y\hat{a}} + \begin{bmatrix} \phi(d)(K_{ft} - K_{dt}v_t) \\ -K_n d^n - K_{dn}\dot{d} \end{bmatrix} = \boldsymbol{Y\hat{a}} + \boldsymbol{F_{total}} \quad (28)$$

TABLE 1: HUMAN LEG PARAMETERS

l_1	Length of the thigh link	0.494	m
l_2	Length of the shank link	0.405	m
m_1	Mass of the thigh link	9.954	kg
m_2	Mass of the shank link	5.063	kg
p_1	Position of the COM along the length of the thigh link	0.202	m
p_2	Position of the COM along the length of the shank link	0.170	m
c_1	Position of the COM perpendicular to the thigh link	-0.050	m
c_2	Position of the COM perpendicular to the shank link	-0.050	m
I_1	Moment of Inertia of thigh link about its COM	0.148	kg-m^2
I_2	Moment of Inertia of shank link about its COM	0.052	kg-m^2
g	Acceleration due to gravity	9.810	m/s^2

We choose the following Lyapunov candidate:

$$V(\boldsymbol{p}, d, \tilde{\boldsymbol{a}}) = \frac{1}{2}\boldsymbol{p}^T \boldsymbol{A} \boldsymbol{p} + \frac{1}{n+1} K_n d^{n+1} + \frac{1}{2}\tilde{\boldsymbol{a}}^T \boldsymbol{P}^{-1} \tilde{\boldsymbol{a}} \quad (29)$$

Here, $\boldsymbol{A}$ is the mass matrix of task space dynamic equations in frame O_p as given in in previous section. $\mathbf{P}^{-1}$ is a positive definite constant matrix and $\tilde{\boldsymbol{a}}$ is the error in parameter estimation defined as:

$$\tilde{\boldsymbol{a}} = \hat{\boldsymbol{a}} - \boldsymbol{a} \quad (30)$$

It can be seen that $V(\mathbf{0},0,\mathbf{0})$=0 and also that V is positive definite. Now, lets differentiate the Lyapunov candidate.

$$\begin{aligned} \dot{V} &= \boldsymbol{p}^T \boldsymbol{A}\dot{\boldsymbol{p}} + \frac{1}{2}\boldsymbol{p}^T \dot{\boldsymbol{A}} \boldsymbol{p} + K_n d^n \dot{d} + \dot{\hat{\boldsymbol{a}}}^T \boldsymbol{P}^{-1} \tilde{\boldsymbol{a}} \\ &= \boldsymbol{p}^T \boldsymbol{A}\dot{\boldsymbol{v}}_{\boldsymbol{m}} + \frac{1}{2}\boldsymbol{p}^T \dot{\boldsymbol{A}} \boldsymbol{p} + K_n d^n \dot{d} + \dot{\hat{\boldsymbol{a}}}^T \boldsymbol{P}^{-1} \tilde{\boldsymbol{a}} \\ &= \boldsymbol{p}^T (\boldsymbol{F} - \boldsymbol{H_p v_m} - \boldsymbol{G_p}) + \frac{1}{2}\boldsymbol{p}^T \dot{\boldsymbol{A}} \boldsymbol{p} + K_n d^n \dot{d} \\ &\quad + \dot{\hat{\boldsymbol{a}}}^T \boldsymbol{P}^{-1} \tilde{\boldsymbol{a}} \\ &= \boldsymbol{p}^T \left(\boldsymbol{F} - \boldsymbol{H_p} \begin{bmatrix} c \\ 0 \end{bmatrix} - \boldsymbol{G_p}\right) + \frac{1}{2}\boldsymbol{p}^T (\boldsymbol{A} - 2\boldsymbol{H_p})\boldsymbol{p} \\ &\quad + K_n d^n \dot{d} + \dot{\hat{\boldsymbol{a}}}^T \boldsymbol{P}^{-1} \tilde{\boldsymbol{a}} \end{aligned}$$

Substitute the control law given by Eq. 26 in the above equations, we get:

$$\begin{aligned} \dot{V} &= \boldsymbol{p}^T \left(\boldsymbol{Y\hat{a}} + \begin{bmatrix} \phi(d)(K_{ft} - K_{dt}v_t) \\ -K_n d^n - K_{dn}\dot{d} \end{bmatrix} - \boldsymbol{H_p} \begin{bmatrix} c \\ 0 \end{bmatrix} - \boldsymbol{G_p}\right) \\ &\quad + K_n d^n \dot{d} + \dot{\hat{\boldsymbol{a}}}^T \boldsymbol{P}^{-1} \tilde{\boldsymbol{a}} \\ &= \boldsymbol{p}^T \left(\boldsymbol{Y\hat{a}} + \begin{bmatrix} \phi(d)(K_{ft} - K_{dt}v_t) \\ -K_n d^n - K_{dn}\dot{d} \end{bmatrix} - \boldsymbol{Ya}\right) \\ &\quad + K_n d^n \dot{d} + \dot{\hat{\boldsymbol{a}}}^T \boldsymbol{P}^{-1} \tilde{\boldsymbol{a}} \\ &= -K_{dt}\phi(d)(v_t - c)^2 - K_{dn}\dot{d}^2 + \boldsymbol{p}^T \boldsymbol{Y}\tilde{\boldsymbol{a}} + \dot{\hat{\boldsymbol{a}}}^T \boldsymbol{P}^{-1} \tilde{\boldsymbol{a}} \end{aligned}$$

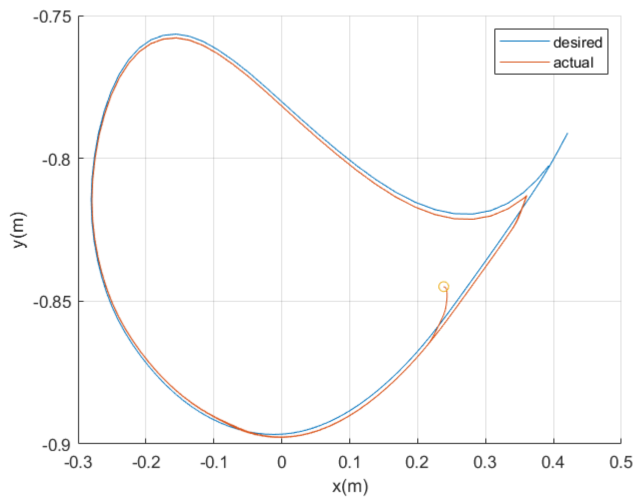

FIGURE 6: PLOT OF DESIRED AND ACTUAL GAIT TRAJECTORY FOR APPROXIMATELY 3 CYCLES

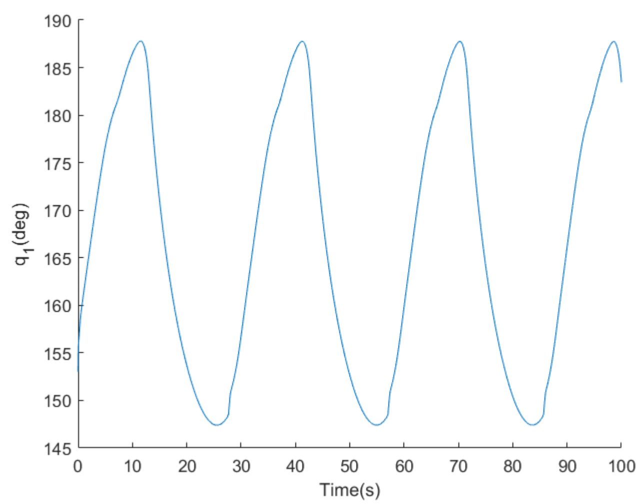

FIGURE 7: ANGULAR POSITION OF THE THIGH LINK FOR THE ACTUAL GAIT TRAJECTORY IN FIG. 6

Now if the following condition holds true:

$$\boldsymbol{p}^T \boldsymbol{Y}\tilde{\boldsymbol{a}} + \dot{\hat{\boldsymbol{a}}}^T \boldsymbol{P}^{-1}\tilde{\boldsymbol{a}} = 0 \tag{31}$$

We have:

$$\dot{V} = -K_{dt}\phi(d)(v_t - c)^2 - K_{dn}\dot{d}^2 \tag{32}$$

If this is satisfied the lyapunov function becomes negative semi-definite and hence the system will be stable. Therefore, we get an adaption law given by Eq.33.

$$\dot{\hat{\boldsymbol{a}}} = -\boldsymbol{P}^T \boldsymbol{Y}^T \boldsymbol{p} \tag{33}$$

This adaptation law was used in simulations of exoskeleton model. The torques at the joints are given by pre-multiplying $J^T R$. Therefore, we finally have the following control law and the adaptation law which constitute our control strategy.

$$\boldsymbol{F} = \boldsymbol{Y}\hat{\boldsymbol{a}} + \begin{bmatrix} \phi(d)(K_{ft} - K_{dt}v_t) \\ -K_n d^{-} K_{dn}\dot{d} \end{bmatrix} = \boldsymbol{Y}\hat{\boldsymbol{a}} + \boldsymbol{F_{total}} \tag{34}$$

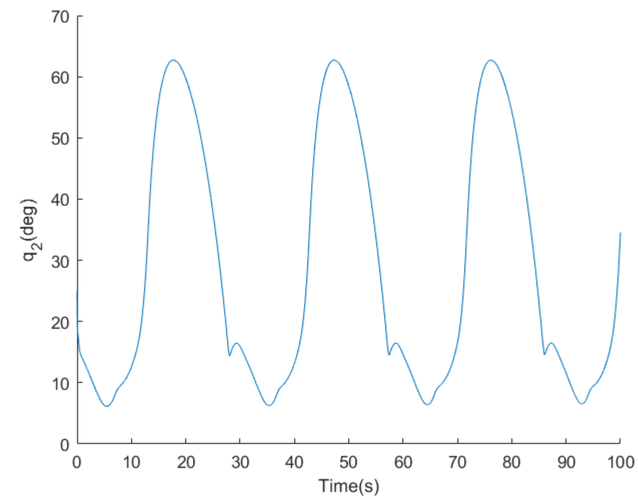

FIGURE 8: ANGULAR POSITION OF THE SHANK LINK FOR THE ACTUAL GAIT TRAJECTORY IN FIG. 6

$$\dot{\hat{\boldsymbol{a}}} = -\boldsymbol{P}^T \boldsymbol{Y}^T \boldsymbol{p} \tag{35}$$

The torques required at the joints are given by:

$$\boldsymbol{\tau} = \boldsymbol{J}^T \boldsymbol{R}\boldsymbol{Y}\boldsymbol{a} + \boldsymbol{J}^T \boldsymbol{R}\boldsymbol{F_{total}} \tag{36}$$

Here, first we get $\boldsymbol{F_{total}}$ in frame 0 by pre-multiplying $\mathbf{R}$ and then multiply by $\mathbf{J^T}$ to get the torques.

4. RESULTS AND CONCLUSIONS

The dynamic model of the leg and exoskeleton was simulated along the adaptive force field controller. In the simulations, healthy subject's average gait data was used to get the desired trajectory [12]. Table 1 shows the inertial parameters used for simulations. This data is a combination of the inertial parameters of the exoskeleton and the data of an average human being [15]. Figure 6 shows the plot of the desired trajectory and multiple cycles of the gait achieved by the exoskeleton model using the adaptive assist as needed control strategy. It can be observed from how close the actual and the desired trajectory are that p apart from being just bounded is also very small. From the simulations, it was found that when the large errors have been reduced and the trajectory starts becoming close to the desired, d is of the order 10^{-3}. Figure 7 and Fig. 8 show the angular positions, q_1 and q_2 of the links. The controller parameters used for these simulations are: $K_{ft} = 90, K_{dn} = 17000, K_{dt} = 2000, D_n = 0.0004, D_t = 0.01, n = 3$. Figure 5 shows the plot of the normal forces, $\boldsymbol{F_n}$ and the perpendicular distance d and Fig. 5 shows the plot of the tangential forces, $\boldsymbol{F_n}$ and the perpendicular distance d. The controller parameters used to get the plots in Fig. 5 are $K_{ft} = 100$, $K_{dt} = 25$, $K_{dn} = 50$, $D_t = 0.005$, $D_n = 0.0025$ and $n = 3$. To clearly demonstrate that the controller is able to reduce a large range of initial errors from the desired trajectory, we simulated the controller with different initial errors and starting points along the desired trajectory. And Figures 9, 10, and 11 show these simulation results where the error is reducing to reasonable small values. The controller parameters used for these

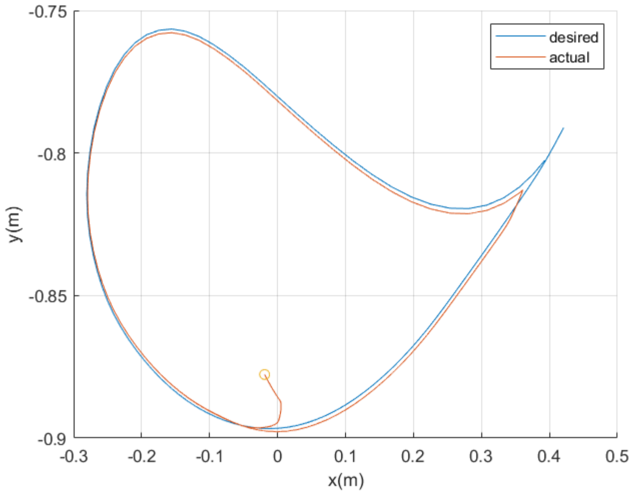

FIGURE 9: CONTROLLER SIMULATION SHOWING TRAJECTORY TRACKING. INITIAL CONFIGURATION OF THE LEG: $q_1 = 170^o$, $q_2 = 25^o$ WITH $d = 0.0189m$

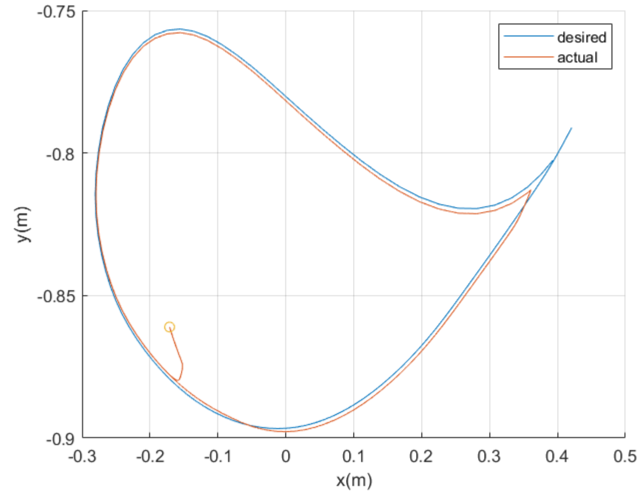

FIGURE 10: CONTROLLER SIMULATION SHOWING TRAJECTORY TRACKING. INITIAL CONFIGURATION OF THE LEG: $q_1 = 180^o$, $q_2 = 25^o$ WITH $d = 0.0177m$

simulations are: $K_{ft} = 90, K_{dn} = 17000, K_{dt} = 2000, D_n = 0.0004, D_t = 0.01, n = 3$.

This paper presents an adaptive force field control strategy for lower limb exoskeletons. The Force Field controller is such that it creates a virtual force field around the foot which gently aids the leg of the user to the desired trajectory. Here the aim is not to achieve perfect tracking but to just assist the leg. However, when there is no user activity ideally the leg should follow the desired trajectory with a constant speed. This property is used to develop a proof for asymptotic stability of the controller. Later this proof is used to design an adaptive control strategy. Using the Lyapunov Stability analysis, an adaptation law which provides an estimate of the unknown parameters is derived. Using this assist as needed controller and the adaptation law, a force field is created around the foot and we are able to achieve a good tracking of the desired trajectory without the knowledge of inertial parameters of the user or the exoskeleton such as mass, inertia, location of COM, etc. We are currently designing a physical prototype of a leg exoskeleton to implement this control strategy on actual hardware. Figure 12 shows the first prototype of the leg exoskeleton developed in the lab.

ACKNOWLEDGMENTS

The authors gratefully acknowledge financial support for this work from Portescap India Private Limited, Mumbai, India through their Corporate Social Responsibility Program. The authors would also like to thank Mr. Pavan Mantripragada, a former research fellow at Indian Institute of Technology Bombay for assistance during early stages of this work.

REFERENCES

[1] Banala, Sai K., Agrawal, Sunil K., Kim, Seok Hun and Scholz, John P. "Novel Gait Adaptation and Neuromotor Training Results Using an Active Leg Exoskeleton." *IEEE/ASME Transactions on Mechatronics* Vol. 15 No. 2 (2010): pp. 216–225. DOI 10.1109/TMECH.2010.2041245.

[2] Colombo, Gery, Jörg, Matthias, Schreier, R and Dietz, Volker. "Treadmill training of paraplegic patients using a robotic orthosis." *Journal of rehabilitation research and development* Vol. 37 (2000): pp. 693–700.

[3] "Robotics Trends. (N/A). ReWalk person exoskeleton. Available :." https://www.roboticsbusinessreview.com/slideshow/rewalk_personal_exoskeleton/. Accessed: 2010-09-30.

[4] Gardner, Amy D., Potgieter, Johan and Noble, Frazer K. "A review of commercially available exoskeletons' capabilities." *2017 24th International Conference on Mechatronics and Machine Vision in Practice (M2VIP)*: pp. 1–5. 2017. DOI 10.1109/M2VIP.2017.8211470.

[5] Etenzi, Ettore, Borzuola, Riccardo and Grabowski, Alena M. "Passive-elastic knee-ankle exoskeleton reduces the metabolic cost of walking." *Journal of NeuroEngineering and Rehabilitation* Vol. 17.

[6] Bridger, Robert, Ashford, Anthea, Wattie, Sarah, Pisula, Peter and Dobson, Karen. "Sustained attention when squatting with and without an exoskeleton for the lower limbs." *International Journal of Industrial Ergonomics* Vol. 66. DOI 10.1016/j.ergon.2018.03.005.

[7] Peternel, Luka, Noda, Tomoyuki, Petrič, Tadej, Ude, Aleš, Morimoto, Jun and Babič, Jan. "Adaptive Control of Exoskeleton Robots for Periodic Assistive Behaviours Based on EMG Feedback Minimisation." *PLOS ONE* Vol. 11 No. 2 (2016): pp. 1–26. DOI 10.1371/journal.pone.0148942. URL https://doi.org/10.1371/journal.pone.0148942.

[8] Li, Zhijun, Huang, Zhicong, He, Wei and Su, Chun-Yi. "Adaptive Impedance Control for an Upper Limb Robotic Exoskeleton Using Biological Signals." *IEEE Transactions on Industrial Electronics* Vol. 64 No. 2 (2017): pp. 1664–1674. DOI 10.1109/TIE.2016.2538741.

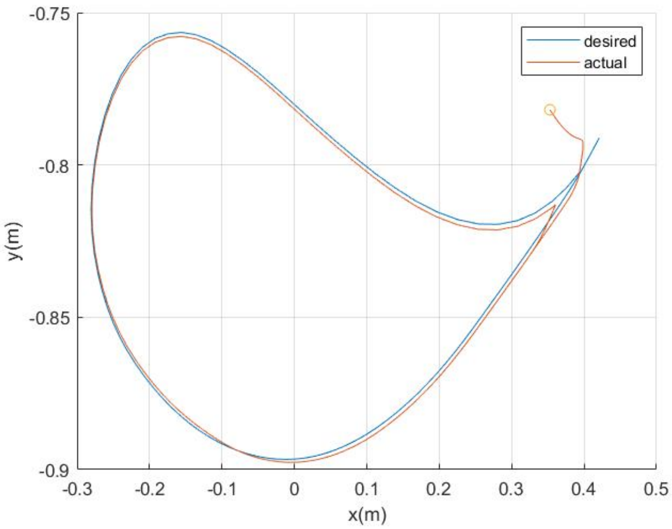

FIGURE 11: CONTROLLER SIMULATION SHOWING TRAJECTORY TRACKING. INITIAL CONFIGURATION OF THE LEG: $q_1 = 180^o$, $q_2 = 35^o$ WITH $d = 0.03m$

[9] Proietti, Tommaso, Jarrassé, Nathanaël, Roby-Brami, Agnès and Morel, Guillaume. "Adaptive control of a robotic exoskeleton for neurorehabilitation." *2015 7th International IEEE/EMBS Conference on Neural Engineering (NER)*: pp. 803–806. 2015. DOI 10.1109/NER.2015.7146745.

[10] Banala, Sai K., Agrawal, Suni K. and Scholz, John P. "Active Leg Exoskeleton (ALEX) for Gait Rehabilitation of Motor-Impaired Patients." *2007 IEEE 10th International Conference on Rehabilitation Robotics*: pp. 401–407. 2007. DOI 10.1109/ICORR.2007.4428456.

[11] Souza, Rafael Sanchez, de Castro Martins, Thiago, Furtado, Guilherme Phillips and Forner-Cordero, Arturo. "Model Reference Adaptive Impedance Controller Design For Modular Exoskeleton." *IFAC-PapersOnLine* Vol. 51 No. 27 (2018): pp. 345–349. DOI https://doi.org/10.1016/j.ifacol.2018.11.616. URL https://www.sciencedirect.com/science/article/pii/S2405896318333251. 10th IFAC Symposium on Biological and Medical Systems BMS 2018.

[12] Bovi, Gabriele, Rabuffetti, Marco, Mazzoleni, Paolo and Ferrarin, Maurizio. "A multiple-task gait analysis approach: Kinematic, kinetic and EMG reference data for healthy young and adult subjects." *Gait posture* Vol. 33 (2011): pp. 6–13. DOI 10.1016/j.gaitpost.2010.08.009.

[13] Spong, Mark W and Vidyasagar, Mathukumalli. *Robot dynamics and control*. John Wiley & Sons (2008).

[14] Slotine, Jean-Jacques E, Li, Weiping et al. *Applied nonlinear control*. Vol. 199. Prentice hall Englewood Cliffs, NJ (1991).

[15] Chandler, R., Clauser, C., McConville, J., Reynolds, Herbert and Young, J. "Investigation of Inertial Properties of the Human Body." (1975): p. 171.

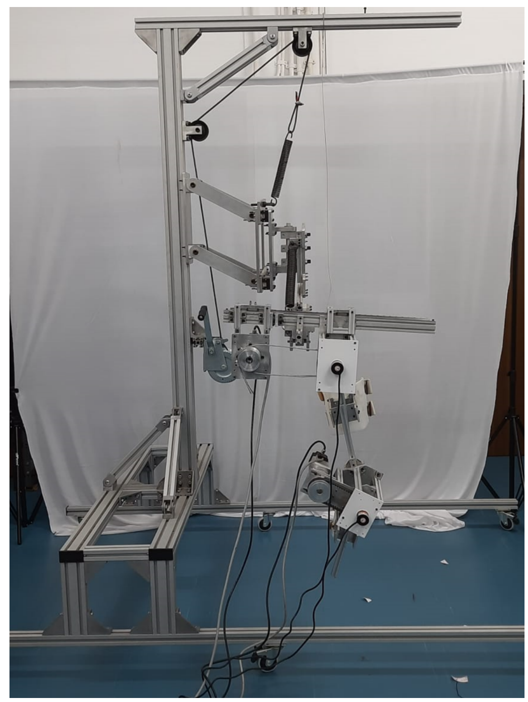

FIGURE 12: PHYSICAL LEG EXOSKELETON